PHYSICAL REVIEW B **93**, 201107(R) (2016)

Isolated energy level in the band gap of $Yb_2Si_2O_7$ identified by electron energy-loss spectroscopy

Takafumi Ogawa,[1,*] Shunsuke Kobayashi,[1] Masashi Wada,[2] Craig A. J. Fisher,[1] Akihide Kuwabara,[1] Takeharu Kato,[1] Masato Yoshiya,[3] Satoshi Kitaoka,[2] and Hiroki Moriwake[1]

[1]*Nanostructures Research Laboratory, Japan Fine Ceramics Center, Nagoya 456-8587, Japan*

[2]*Materials Research and Development Laboratory, Japan Fine Ceramics Center, Nagoya 456-8587, Japan*

[3]*Department of Adaptive Machine Systems, Osaka University, Osaka 565-0871, Japan*

(Received 8 April 2016; published 18 May 2016)

We report the detection of an isolated energy level in the band gap of crystalline $Yb_2Si_2O_7$ in the low-energy-loss region of its electron energy-loss (EEL) spectrum, obtained using a monochromated scanning transmission electron microscope. The experimental results are corroborated by first-principles calculations of the theoretical EEL spectrum. The calculations reveal that unoccupied Yb $4f$ orbitals constitute an isolated energy level about 1 eV below the conduction band minimum (CBM), resulting in a terrace about 1 eV wide at the band edge of the EEL spectrum. In the case of Yb_2O_3, no band edge terrace is present because the unoccupied f level lies just below the CBM. We also examined optical absorption properties of $Yb_2Si_2O_7$ using UV-vis diffuse reflectance spectroscopy, which shows that the isolated energy level could not be detected in the band edge of the obtained absorbance spectrum. These findings demonstrate the utility of low-loss EEL spectroscopy with high energy resolution for probing semilocalized electronic features.

DOI: 10.1103/PhysRevB.93.201107

Valence electron energy-loss (EEL) spectroscopy for loss energies less than about 50 eV using a scanning transmission electron microscope (STEM) [1] has been developed into a powerful analysis method to investigate low-energy ($\leqslant$50 eV) excitation in solids with nanoscale spatial resolution. The majority of valence EEL studies to date have looked at plasmon peaks, band gaps, and dielectric functions in bulk materials [2–8], as well as nanotubes [9], nanoclusters [10], heterostructure interfaces [11,12], graphene sheets [13,14], and quantum dots [15]. Valence EEL spectroscopy has also been used to measure nanoscale strain based on shifts of plasmon peaks [16,17] and vibrational properties [18]. Although similar improvements have recently been achieved in reflection EEL spectroscopy [19,20], valence EEL spectroscopy with STEM still has the advantage in terms of higher spatial resolution and is less influenced by surface effects. In this paper, we report a previously unknown isolated energy level in the band gap of $Yb_2Si_2O_7$, which appears at the edge of the EEL spectrum, as well as the theoretical spectrum based on density functional theory (DFT). For reference and comparison, we also investigated ytterbium sesquioxide, Yb_2O_3, using the same methods.

Except for the two end members, La and Lu, rare-earth elements Ln in sesquioxides contain partially occupied $4f$ orbitals. Optical measurements [21,22] and DFT-based calculations [23–25] have revealed that band gaps of Ln_2O_3 vary systematically with atomic number, with two dips in each half of the Ln series. In these systems, while valence and conduction bands are composed of O $2p$ and Ln $5d$ orbitals, respectively, Ln $4f$ orbitals participate in the formation of the side bands and isolated levels within the gap. In the case of Yb^{3+} with 13 $4f$ electrons, the occupied f orbitals are buried under the valence band maximum (VBM) and the unoccupied f orbital settles slightly below the conduction band minimum (CBM), producing a band gap that corresponds to one of these dips.

The $Ln_2Si_2O_7$ series also exhibits structural variations [26], but little is known about the electronic structures of each member. Pidol *et al.* reported an x-ray photoemission spectroscopy (XPS) and inverse XPS study of Ln-doped $Lu_2Si_2O_7$, and an XPS study of single-crystal $Yb_2Si_2O_7$ aimed at investigating electronic structures of these materials [27]. They found that (a) the band gap in the case of the Lu silicate, with fully occupied f orbitals, was 7.8 eV, significantly larger than the gap of 5.5 eV in Lu_2O_3 [22], and (b) for $Yb_2Si_2O_7$, occupied f-orbital levels are about 1.0 eV below the VBM and overlap with O p orbitals. Because the $4f$ levels of Ln compounds vary systematically across the period [28], determining f orbital positions and host p-d band gaps for a single case can aid prediction of as-yet-unknown optical properties of other Ln compounds for applications such as phosphors and lasers. In this paper, we show how valence EEL spectroscopy can be utilized for measuring such electronic properties of Ln compounds.

To prepare $Yb_2Si_2O_7$ sample powders, spray pyrolyzed powders, starting from silica sol (ST-OXS, Nissan Chemical Industries, Ltd.) and $Yb(NO_3)_3 \cdot xH_2O$ (99.9% purity, Nippon Yttrium Co., Ltd), were calcined at 1300°C for 2 hrs in air. Powders consisted of the β phase [26] with space group $C2/m$, as confirmed by x-ray diffraction [29]. The Yb/Si ratio was confirmed to be 1.00 by inductively coupled plasma atomic emission spectroscopy. For the sesquioxide, 99.9% purity Yb_2O_3 powders (Advantec Co., Ltd.) of the stable bixbyite phase (space group $Ia\bar{3}$) were used.

TEM samples were prepared from crushed particles supported on holey carbon films. EEL spectra were obtained using an EEL spectrometer (Tridiem ERS, Gatan, Inc.) attached to an aberration-corrected (CEOS GmbH) STEM (JEM-2400FCS, JEOL Ltd.) operated at 60 kV with a Wien filter monochromator. EEL spectra were recorded within a rectangular area (about 3 nm × 3 nm) in STEM mode, using 0.05 eV per channel and an energy resolution of less than 150 meV (full-width at half-maximum of the zero-loss peak).

Figures 1(a) and 1(b) show EEL spectra for Yb_2O_3 and $Yb_2Si_2O_7$, respectively. While a sharp plasmon peak centered

*t_ogawa@jfcc.or.jp

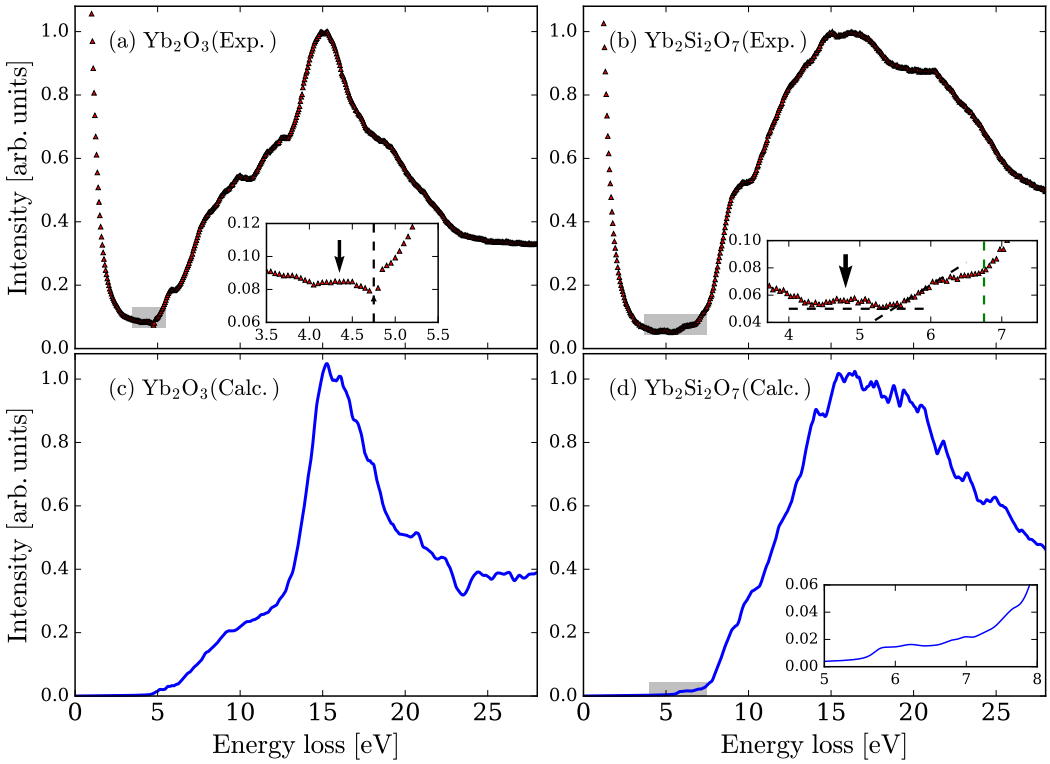

FIG. 1. Experimental electron energy loss spectra of (a) Yb_2O_3 and (b) $Yb_2Si_2O_7$ and calculated electron energy loss spectra of (c) Yb_2O_3 and (d) $Yb_2Si_2O_7$. Insets in Figs. (a), (b), and (d) show magnified views of the band-edge regions enclosed by the gray shaded boxes.

at 15 eV is found for Yb_2O_3 [Fig. 1(a)], the plasmon peak of $Yb_2Si_2O_7$ is broad and extends over a range from 14 eV to 22 eV [Fig. 1(b)]. The latter may be a result of overlapping of two peaks centered at 15 eV and 22 eV. The spectrum of Yb_2O_3 has a steep edge at 4.75 eV, indicated by the vertical line in the inset of Fig. 1(a), consistent with the band gaps of 4.9 eV [21] and 5.05 eV [22] obtained by optical measurements, and 4.7 eV obtained from the many-body perturbation calculations based on the local density approximation (LDA) with a Hubbard-type correction, GW_0@LDA + U [24]. In contrast, the band edge of $Yb_2Si_2O_7$ consists of a low terrace with an energy width of about 1 eV [the inset of Fig. 1(b)]. In addition, weak peaks at around 4.5 eV under the band edges are found in both cases, indicated by arrows in the insets of Figs. 1(a) and 1(b).

In order to determine the optical band gap of $Yb_2Si_2O_7$, we took UV-vis diffuse reflectance spectra (DRS) with a Parkin Elmer Lambda-950 spectrophotometer equipped with a 150 mm integrating sphere accessory using $BaSO_4$ reflectance standards. The obtained reflectance, R_∞, was used in a Tauc plot, $(h\nu F(R_\infty))^{1/r}$ [30], via the Kublka-Munk function (absorbance), $F(R_\infty) = (1 - R_\infty)^2/2R_\infty$, where r is determined by transition type. Since the charge transfer (CT) excitation mechanism has been reported for Yb_2O_3 [21,28] and doped Yb atoms in an isostructural host material, $Lu_2Si_2O_7$ [27], we here assume the CT transition, leading to an allowed transition. In addition, our band structure calculations indicate a direct gap [29]. Consequently, we used $r = 1/2$ for the Tauc plot in Fig. 2. The resulting optical gap is 5.6 eV, close to the edge of the weak terrace in the $Yb_2Si_2O_7$ EEL spectrum and larger by 0.85 eV than that of Yb_2O_3. It should be noted that no signal corresponding to the wide weak terrace in the EEL spectrum was found in the optical spectrum.

The experimental results can be interpreted in light of DFT calculations performed using the projector augmented wave (PAW) method [31] implemented in the ABINIT code [32,33]. For the exchange-correlation functional, the Perdew-Barck-Ernzahoff (PBE) generalized gradient approximation (GGA) was used [34]. We used the PAW data sets in the JTH-v0.2 library [35] for Si and O atoms, and one provided by Topsakal and Wentzcovitch [36] for Yb atoms. The DFT + U scheme

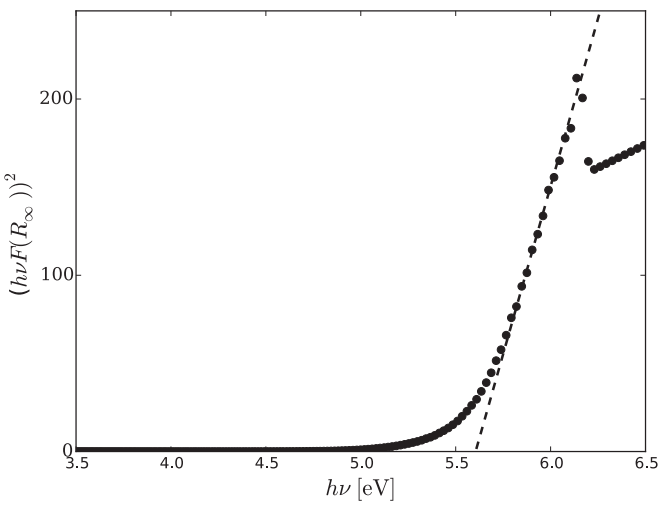

FIG. 2. Absorbance spectrum of $Yb_2Si_2O_7$ generated from the diffuse reflectance spectrum.

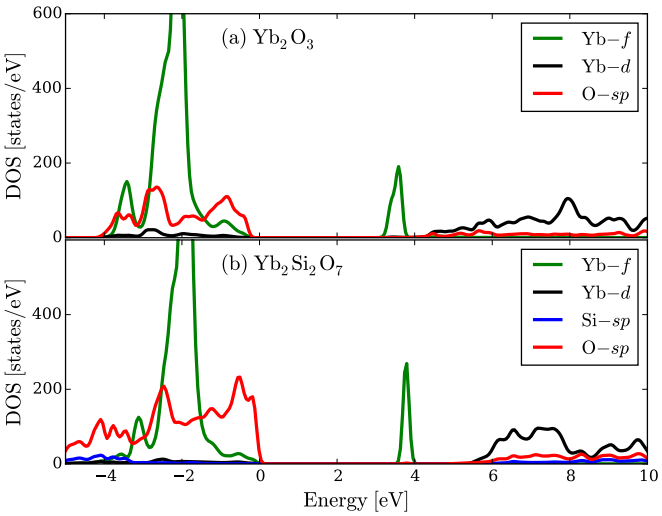

FIG. 3. Electronic density of states (DOS) in (a) Yb_2O_3 and (b) $Yb_2Si_2O_7$. The horizontal axes indicate the energy relative to the valence band maximum.

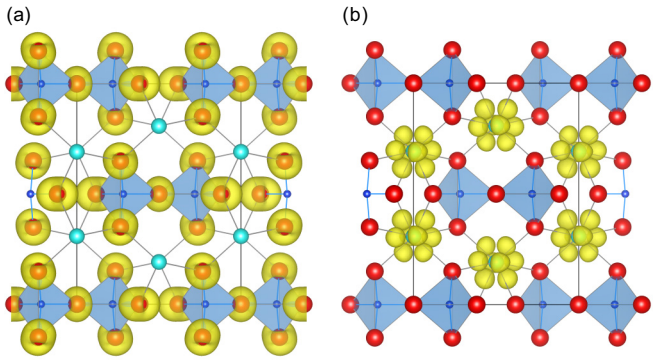

FIG. 4. Partial electronic charge densities of $Yb_2Si_2O_7$ belonging to (a) the 0.9 eV wide energy region beneath the valence band minimum and (b) the isolated energy levels in the band gap. The blue tetrahedra and cyan spheres in the interstitial regions of the tetrahedra represent SiO_4 units and Yb atoms, respectively.

was used for f orbitals in Yb atoms with the around-mean field double counting term [37,38]. The U-ramping method was used to obtain the ground-state electronic structures [39]. A value of $U = 6$ eV was selected, producing a similar electronic structure to that of GW_0@LDA + U calculations of Yb_2O_3 [24]. The Brillouin zone was sampled using Γ-centered Monkhorst-Pack grids [40] with mesh widths less than 0.3 $Å^{-1}$ in each direction; a plane-wave cutoff energy of 544 eV (20 Ha) was used in all cases. Dielectric functions (and EEL functions) were calculated using the independent particle approximation, i.e., random phase approximation (RPA), without local field effects. The primitive cells contained 40 and 11 atoms in the case of Yb_2O_3 and $Yb_2Si_2O_7$, respectively. The optimized structures and dependences of band gaps on U are provided as Supplemental Material [29].

The calculated electronic densities of states (DOS) are shown in Fig. 3. The valence bands of Yb_2O_3 are mainly composed of O $2p$ and Yb $4f$, and the conduction bands of Yb $5d$ and Yb $4f$, where the position of unoccupied Yb $4f$ levels is just below the Yb $5d$ band minimum, consistent with the results of previous experiments [21,22,28] and GW_0@LDA + U calculations [24]. The calculated band gap of 3.39 eV is, however, significantly less than experimental values of 4.75–5.1 eV, due to persistent underestimation of the p-d gap commonly seen in GGA and LDA calculations. The DOS of $Yb_2Si_2O_7$ shows a similar structure to that of Yb_2O_3; the valence band is relatively wide due to resonance between Si and O orbitals in the region below −4 eV, and the Yb $5d$ conduction band is shifted toward a higher energy region than in the case of Yb_2O_3 by about 1.1 eV. This leads to the formation of the isolated energy level at 0.9 eV below the Yb $5d$-band bottom. The resulting band gap of 3.77 eV is also much lower than the optically measured value of 5.6 eV. In the following dielectric function calculations, we applied scissor shifts for all unoccupied levels to adjust the optical gaps.

The theoretical EEL functions, $-\mathrm{Im}[\varepsilon^{-1}]$, in Figs. 1(c) and 1(d) were extracted from the calculated dielectric functions ε. A plasmon peak centered at 15 eV of Yb_2O_3 is seen in Fig. 1(c), consistent with the experimental spectrum. For $Yb_2Si_2O_7$, the calculated plasmon signals also consistently exhibit a wide plateau over 15–20 eV as seen in Fig. 1(d). Since the energy levels of Si-O bonding are formed in a lower energy region than Yb-O bonding levels in the valence band [Fig. 3(b)], the plateaulike feature of the plasmon peak may originate from the Si-O bonding contribution overlapping with the Yb-O contribution. The shoulders at around 10 eV in both the experimental EEL spectra in Figs. 1(a) and 1(b) are missing in the calculated spectra. These are thought to correspond to surface plasmons, which are absent from our bulk calculations. The surface plasmon peak, E_{sp}, can be estimated from the bulk plasmon peak, $E_p = 15.0$ eV, according to $E_{sp} = E_p/\sqrt{2}$ under the free electron approximation [1], which gives a value of 10.6 eV.

The calculated EEL spectrum of $Yb_2Si_2O_7$ in Fig. 1(d) confirms the experimentally observed weak terrace of about 1 eV in width; in both cases the terrace heights are less than 10% those of the plasmon peak maxima. As revealed by the DOS, the terrace corresponds to an interband transition from the O orbitals near the VBM to the isolated energy level of the unoccupied $4f$ orbitals. The partial charge densities belonging to the VBM region 0.9 eV in width and the isolated levels in the gap in Fig. 4 exhibit localized distributions centered on O and Yb atoms, respectively. Although beyond the scope of this study, this suggests the terrace region can be used to investigate the spatial distribution of the excitation on the atomistic scale, i.e., spectrum images, uniquely by EEL spectroscopy attached to an STEM.

The rise from the terrace at 6.75 eV in the experimental EEL spectrum of $Yb_2Si_2O_7$, indicated by the vertical line in the inset of Fig. 1(b), corresponds to the transition from the valence band to the Yb $5d$ band, i.e., the p-d gap. This is larger than the p-d gap of Yb_2O_3, near to the p-f gap of 4.75 eV. Our calculations also indicate a similar tendency where the p-d gap of $Yb_2Si_2O_7$ is larger by about 1.1 eV than that of Yb_2O_3 as in Fig. 3. According to the model proposed by van der Kolk and Dorenbos [28], the $5d$ bands of Ln in $Ln_2Si_2O_7$ should be shifted upwards in all cases compared to Ln_2O_3, as evidenced by XPS studies of Lu systems: The p-d gap of 7.8 eV in $Lu_2Si_2O_7$ is larger than that of 5.5 eV in Lu_2O_3 [27].

The calculated optical absorption spectrum, Im[ε], of $Yb_2Si_2O_7$ also has a weak terrace at the edge similar to the EEL spectrum [29]. The experimental spectrum in Fig. 2, however, exhibits no corresponding signal. This discrepancy is not surprising as similar situations commonly occur in semiconductors and insulators, where coupling effects of electrons and holes need to be included in theoretical models using more sophisticated methods, e.g., many-body perturbation approaches dealing with the Bethe-Salpeter equation and time-dependent DFT [41] even for qualitative reproduction of experimental optical absorption data. The origin of the smeared feature in our optical measurement is expected to be the effect of these excitons, which shifts the spectrum signals towards the lower energy region.

The weak peaks below the band edges in both Yb_2O_3 and $Yb_2Si_2O_7$ EEL spectra cannot be interpreted from our calculations. As already seen in the case of $Yb_2Si_2O_7$, isolated levels in the band gap contribute to such signals with small intensity under the band edge. This leads us to suppose that point defects are the origin of these signals because defect transition levels are known to emerge in the gaps of insulating solids. For example, similar signals in the reflection EEL spectrum of MgO were attributed to oxygen vacancies [19]. Since it is possible that the signals vary with the amount of incident electron beam damage, these peaks cannot be attributed definitively to intrinsic processes in the materials. These findings may, therefore, mean that characterization of isolated levels by valence EEL spectroscopy is limited, for example, to systems with semilocalized atomic orbitals, such as are found in the Ln compounds investigated here or in transition metal impurities in semiconductors.

In summary, we have shown using EEL spectroscopy and DFT calculations that the weak terrace about 1 eV in width at the band edge corresponds to an isolated energy level in the band gap of $Yb_2Si_2O_7$. This terrace is caused by electron excitation from the valence band top to spatially localized Yb $4f$ orbitals. In addition, the EEL spectra suggest that the p-d gap of $Yb_2Si_2O_7$ is large compared to that of Yb_2O_3. This study shows how a combination of valence EEL spectroscopy with high energy resolution and DFT calculations of EEL spectra on the RPA level provides an alternative method to optical absorption spectroscopy for analyzing electronic structures of semiconductors and insulators.

This work was partly supported by the Council for Science, Technology and Innovation (CSTI), Cross-ministerial Strategic Innovation Promotion Program (SIP), "Structural Materials for Innovation" from Japan Science and Technology Agency, and by Grants-in-Aid for Scientific Research on Innovative Areas "Nano Informatics" (25106008) and KAKENHI (15K18218) from Japan Society for the Promotion of Science.

[1] R. F. Egerton, *Electron Energy-Loss Spectroscopy in the Electron Microscope*, 3rd ed. (Springer, New York, 2011).
[2] V. J. Keast, Appl. Phys. Lett. **79**, 3491 (2001).
[3] V. J. Keast, A. J. Scott, M. J. Kappers, C. T. Foxon, and C. J. Humphreys, Phys. Rev. B. **66**, 125319 (2002).
[4] S. Schamm and G. Zanchi, Ultramicroscopy **96**, 559 (2003).
[5] R. Erni and N. D. Browning, Ultramicroscopy **104**, 176 (2005).
[6] L. Gu, V. Srot, W. Sigle, C. Koch, P. van Aken, F. Scholz, S. B. Thapa, C. Kirchner, M. Jetter, and M. Rühle, Phys. Rev. B **75**, 195214 (2007).
[7] J. Danet, T. Brousse, K. Rasim, D. Guyomard, and P. Moreau, Phys. Chem. Chem. Phys. **12**, 220 (2010).
[8] N. Jiang and J. C. H. Spence, Ultramicroscopy **134**, 68 (2013).
[9] R. Arenal, O. Stéphan, M. Kociak, D. Taverna, A. Loiseau, and C. Colliex, Phys. Rev. Lett. **95**, 127601 (2005).
[10] J. R. Jinschek, R. Erni, N. F. Gardner, A. Y. Kim, and C. Kisielowski, Solid State Commun. **137**, 230 (2006).
[11] P. E. Batson, K. L. Kavanagh, J. M. Woodall, and J. W. Mayer, Phys. Rev. Lett. **57**, 2729 (1986).
[12] A. Y. Borisevich, H. J. Chang, M. Huijben, M. P. Oxley, S. Okamoto, M. K. Niranjan, J. D. Burton, E. Y. Tsymbal, Y. H. Chu, P. Yu, R. Ramesh, S. V. Kalinin, and S. J. Pennycook, Phys. Rev. Lett. **105**, 087204 (2010).
[13] W. Zhou, J. Lee, J. Nanda, S. T. Pantelides, S. J. Pennycook, and J.-C. Idrobo, Nat. Nanotechnol. **7**, 161 (2012).
[14] M. D. Kapetanakis, W. Zhou, M. P. Oxley, J. Lee, M. P. Prange, S. J. Pennycook, J. C. Idrobo, and S. T. Pantelides, Phys. Rev. B **92**, 125147 (2015).
[15] M. Logar, S. Xu, S. Acharya, and F. B. Prinz, Nano Lett. **15**, 1855 (2015).
[16] A. M. Sanchez, R. Beanland, A. J. Papworth, P. J. Goodhew, and M. H. Gass, Appl. Phys. Lett. **88**, 051917 (2006).
[17] J. Palisaitis, C.-L. Hsiao, M. Junaid, J. Birch, L. Hultman, and P. O. Å. Persson, Phys. Rev. B **84**, 245301 (2011).
[18] O. L. Krivanek, T. C. Lovejoy, N. Dellby, T. Aoki, R. W. Carpenter, P. Rez, E. Soignard, J. Zhu, P. E. Batson, M. J. Lagos, R. F. Egerton, and P. A. Crozier, Nature (London) **514**, 209 (2014).
[19] S. Heo, E. Cho, H.-I. Lee, G. S. Park, H. J. Kang, T. Nagatomi, P. Choi, and B.-D. Choi, AIP Adv. **5**, 077167 (2015).
[20] M. Vos, G. G. Marmitt, Y. Finkelstein, and R. Moreh, J. Chem. Phys. **143**, 104203 (2015).
[21] A. V. Prokofiev, A. I. Shelykh, and B. T. Melekh, J. Alloy Compd. **242**, 41 (1996).
[22] S. Kimura, F. Arai, and M. Ikezawa, J. Phys. Soc. Jpn. **69**, 3451 (2000).
[23] H. Jiang, R. I. Gomez-Abal, P. Rinke, and M. Scheffler, Phys. Rev. Lett. **102**, 126403 (2009).
[24] H. Jiang, P. Rinke, and M. Scheffler, Phys. Rev. B **86**, 125115 (2012).
[25] R. Gillen, S. J. Clark, and J. Robertson, Phys. Rev. B **87**, 125116 (2013).
[26] N. Maier, G. Rixecker, and K. G. Nickel, J. Solid State Chem. **179**, 1630 (2006).
[27] L. Pidol, B. Viana, A. Galtayries, and P. Dorenbos, Phys. Rev. B **72**, 125110 (2005).
[28] E. van der Kolk and P. Dorenbos, Chem. Mater. **18**, 3458 (2006).
[29] See Supplemental Material at http://link.aps.org/supplemental/10.1103/PhysRevB.93.201107 for x-ray diffraction data and calculated data such as energy bands, band gaps, lattice constants, and dielectric functions.

[30] J. Tauc, Mater. Res. Bull. **3**, 37 (1968).
[31] M. Torrent, F. Jollet, F. Bottin, G. Zérah, and X. Gonze, Comp. Mater. Sci. **42**, 337 (2008).
[32] X. Gonze, J.-M. Beuken, R. Caracas, F. Detraux, M. Fuchs, G.-M. Rignanese, L. Sindic, M. Verstraete, G. Zerah, F. Jollet, M. Torrent, A. Roy, M. Mikami, P. Ghosez, J.-Y. Raty, and D. C. Allan, Comp. Mater. Sci. **25**, 478 (2002).
[33] X. Gonze, B. Amadon, P. M. Anglade, J.-M. Beuken, F. Bottin, P. Boulanger, F. Bruneval, D. Caliste, R. Caracas, M. Côte, T. Deutsch, L. Genovese, P. Ghosez, M. Giantomassi, S. Goedecker, D. Hamann, P. Hermet, F. Jollet, G. Jomard, S. Leroux, M. Mancini, S. Mazevet, M. J. T. Oliveira, G. Onida, Y. Pouillon, T. Rangel, G.-M. Rignanese, D. Sangalli, R. Shaltaf, M. Torrent, M. J. Verstraete, G. Zerah, and J. W. Zwanziger, Comput. Phys. Commun. **180**, 2582 (2009).
[34] J. P. Perdew, K. Burke, and M. Ernzerhof, Phys. Rev. Lett. **77**, 3865 (1996).
[35] F. Jollet, M. Torrent, and N. Holzwarth, Comput. Phys. Commun. **185**, 1246 (2014).
[36] M. Topsakal and R. M. Wentzcovitch, Comput. Mater. Sci. **95**, 263 (2014).
[37] M. T. Czyżyk and G. A. Sawatzky, Phys. Rev. B **49**, 14211 (1994).
[38] B. Amadon, F. Jollet, and M. Torrent, Phys. Rev. B **77**, 155104 (2008).
[39] B. Meredig, A. Thompson, H. A. Hansen, C. Wolverton, and A. van de Walle, Phys. Rev. B **82**, 195128 (2010).
[40] H. J. Monkhorst and J. D. Pack, Phys. Rev. B **13**, 5188 (1976).
[41] G. Onida, L. Reining, and A. Rubio, Rev. Mod. Phys. **74**, 601 (2002).